J. Cosmet. Sci., 64, 99–110 (March/April 2013)

Inhibitory mechanism of red globe amaranth on tyrosinase

YAN MU, LIN LI, YONG ZHOU, HAI-LIU WEI, and SONG-QING HU, *Guangdong Province Key Laboratory for Green Processing of Natural Products and Product Safety, College of Light Industry and Food Sciences, South China University of Technology, Guangdong 510640, People's Republic of China (Y.M., L.L., H.-L.W., S.-Q.H.) and School of Software Technology, Dalian University of Technology, Liaoning 116024, People's Republic of China (Y.Z.).*

Accepted for publication June 19, 2012.

Synopsis

Tyrosinase inhibitors from natural plants are currently attracting great interest. In this study, vanillic acid (VA) from red globe amaranth flower was identified as an effective tyrosinase inhibitor. The 50% inhibitory concentration values of VA were 0.53 and 0.63 mg/ml for the monophenolase and diphenolase activities of tyrosinase, respectively. VA did not function as a simple copper chelator, and it did not induce detectable changes in the enzyme conformation. An investigation into the interaction between VA and tyrosinase by docking method revealed that VA was bound to residues at the entrance to the dicopper center. This suggests that VA could strongly inhibit tyrosinase activity by hampering the binding of substrates to tyrosinase. Because of the stability of the complex, VA hindered binding of monophenol substrates better than that of diphenol substrates, which resulted in different inhibitory efficacies. A study of the mechanism of tyrosinase inhibition provided new evidence to elucidate the molecular mechanism of depigmentation by red globe amaranth plant.

INTRODUCTION

Melanin plays an important role in skin pigmentation, and it is synthesized from tyrosine by tyrosinase (EC 1.14.18.1). Melanin is widely distributed in nature; it is found in many organisms, including microorganisms, plants and animals; and catalyzes two key reactions in the melanin biosynthesis pathway: the hydroxylation of monophenol to *o*-diphenol (monophenolase activity) followed by the oxidation of *o*-diphenol to the corresponding *o*-quinone (diphenolase activity), which can polymerize spontaneously to form melanins (1–3). It is well documented that tyrosinase is an essential enzyme, and it is thought to be the rate-limiting enzyme in melanin synthesis. (4).

Although the production of melanin in human skin is a major defense mechanism against solar irradiation, the abnormal production of the pigment can lead to melasma, freckles,

Address all correspondence to Song-Qing Hu at fesqhu@scut.edu.cn.

age spots, liver spots, and other types of melanin hyperpigmentation disorders, and it can cause serious aesthetic problems and even diseases such as melanoma (5). In the food industry, tyrosinase activity may generate undesirable browning, which causes deleterious changes such as an unattractive appearance and reduced nutritional quality of the food product (1,6,7). In light of these cosmetic, agricultural, and medicinal problems (8), inhibitors of tyrosinase have attracted great interest as treatments for disorders that are associated with the overproduction of melanin (9). Recently, increased attention has been paid to tyrosinase inhibitors derived from natural plants, which are rich in bioactive chemicals and mostly free of side effects; some of them, such as arbutin (a glycosylated hydroquinone found in certain plants), are already used in the cosmetic industry for skin whitening (10,11).

The red globe amaranth, a cultivar of *Gomphrena globosa*, is a medicinal plant in the Amaranthaceae family. Its flower can be made into a highly valued scented tea. It was used to pay tribute in ancient China because of its ability to whiten skin, especially in the treatment of melasma, freckles, age spots, liver spots, and other forms of melanin hyperpigmentation. Some constitutes, such as betacyanins, flavonoids, and flavonols, have already been isolated from some species of *Gomphrena* (12,13). However, the constituents of red globe amaranth plant that are responsible for whitening and the molecular mechanism of this effect are still unclear. In this study, we identified for the first time that vanillic acid (VA) is one of the primary skin-whitening constituents of red globe amaranth. The inhibitory effect of VA on tyrosinase was investigated by examining enzyme kinetics, group mutations, and ability of inhibiting melanogenesis by melanocyte (14–16). However, until now, the role of the interaction between VA and tyrosinase in the inhibition of tyrosinase remains unknown.

To better understand the inhibition of tyrosinase, we analyzed the spectra and simulated the molecular interaction of VA and tyrosinase. Our study provides new evidence to help elucidate the molecular mechanism of depigmentation by red globe amaranth and helps to facilitate the proper application of this valuable plant.

MATERIALS AND METHODS

MATERIALS

The red globe amaranth originated from Yunnan province in China and was purchased from a local Qingping herbal medicine market. L-tyrosine, L-dopa, and mushroom tyrosinase (EC 1.14.18.1) were purchased from Sigma-Aldrich (St. Louis, MO). All other chemicals were of analytical grade and manufactured in China.

TYROSINASE ACTIVITY ASSAY

This assay was performed using previously described methods (11) with slight modifications. The samples were dissolved in dimethyl sulfoxide and prepared in uniform concentrations for each batch; L-tyrosine and L-dopa served as the monophenol and diphenol substrates, respectively. First, the samples were tested at only a single concentration for

their inhibitory effect on the monophenolase activated forms of tyrosinase *in vitro*. Next, the best sample was selected for a dose–response study for the monophenolase and diphenolase activities of tyrosinase. In a 96-well plate, 70 µl of each dilution of the extract was mixed with 30 µl tyrosinase solution (333 units/ml in phosphate buffer) in triplicate. After incubation at 25°C for 5 min, 110 µl of the substrate (1.0 m*M* L-tyrosine or 2.0 m*M* L-dopa) was added to each well. The samples were incubated for 30 min at 25°C. The optical densities of the samples were then determined at 492 nm using a Sunrise plate reader (TECAN, Männedorf, Switzerland). The concentrations of the inhibitor at which half of the original tyrosinase activity was inhibited (50% inhibitory concentration, IC_{50}) were determined for crude extract and purified inhibitors. Arbutin was selected as a positive control. All concentrations of the inhibitors mentioned in the study were the final concentrations. The inhibition of tyrosinase activity was calculated as follows:

$$\% \text{ Inhibition} = \left[\frac{1-(B-C)}{A}\right] \times 100$$

A is the absorbance at 492 nm without the test sample, *B* the absorbance at 492 nm with the test sample, and *C* the absorbance at 492 nm without tyrosinase.

EXTRACTION OF CRUDE EXTRACT AND PRELIMINARY SEPARATION EXPERIMENT

Dried flowers of red globe amaranth (3 kg) were extracted three times by reflux extraction with a fivefold, 50% (v/v) aqueous alcohol solution; each incubation was performed for 2 h. After filtration through 0.45 µm filter paper, the filtrates were mixed and concentrated using a rotary evaporator (Yarong Inc., Shanghai, China) at 50°C. The concentrated extract was dispersed with distilled water until its density was approximately 1.0–1.1 g/cm^3. Then, the suspended liquid was successively extracted at room temperature four times each by petroleum ether, ethyl acetate, and butanol (1 liter of each solvent, 24 h), and the organic phases were concentrated to produce the extracts, which were termed PE, EA, and BA, respectively. We performed a preliminary experiment for the extracts by crudely separating them using silica gel chromatography. For PE and EA, a petroleum ether–acetic ether mixture was used as the eluent, whereas chloroform–methanol ($CHCl_3$–MeOH) was used as the eluent for BA. The inhibitory effect of the crude separated fractions at 1 mg/ml on tyrosinase activity is listed in Table I; EA was selected for further purification studies.

Table I
Tyrosinase Inhibition by Fractions from PE, EA, and BA

	Tyrosinase inhibition rate (%)									
Fraction	1	2	3	4	5	6	7	8	9	10
PE	—	—	—	16.58	16.38	17.93	10.35	8.70	30.06	—
EA	—	—	30.74	44.01	72.55	92.72	33.79	53.32	33.79	41.68
BA	16.34	17.96	−24.68	−4.94	−1.53	−5.63	−2.08	−9.54	12.42	40.99

PURIFICATION OF THE TYROSINASE INHIBITOR

The purification was based on the tyrosinase activity-guided method. The EA was separated by column chromatography over silica gel with mixtures of petroleum ether–acetic ether of increasing polarity (9:1–4:6), and 14 fractions (A–N) were collected. Fractions A–F were discarded because they were insoluble in our enzyme activity assay, and the remaining 8 fractions were separated over a Sephadex LH-20 (GE Inc., New York, NY) column with $CHCl_3$–MeOH (1:1). The compounds with a high level of tyrosinase inhibition were further refined by C18 (GE Inc.) column chromatography and eluted with methanol aqueous solutions (20%, 40%, 60%, 80%, and 100%, successively) (v/v) to prepare a white powder (approximately 30 mg), which was washed with the 40% methanol eluent. The final yield of the white powder is approximately 0.01%. The overall flow chart of the isolation and purification process is shown in Figure 1.

STRUCTURE DETERMINATION

The structure of the obtained compound was determined using AVANCE Digital 400 MHz NMR Spectrometer (Bruker Inc., Karlsruhe, Germany). The detailed structural information is as follows: ^{1}H-NMR ($CDCl_3$,δ, ppm.) 7.56 (1H, d, J = 4 Hz), 7.54 (1H, d, J = 4 Hz), 6.83 (1H, t, J = 8 Hz), 3.90 (3H, s); ^{13}C-NMR ($CDCl_3$, δ, ppm.) 170.21(s), 152.85(s), 148.85(s), 125.48(d), 123.29(s), 116.04(d), 114.08(d), and 56.63(q). Previous reports (17,18) have identified this compound as VA.

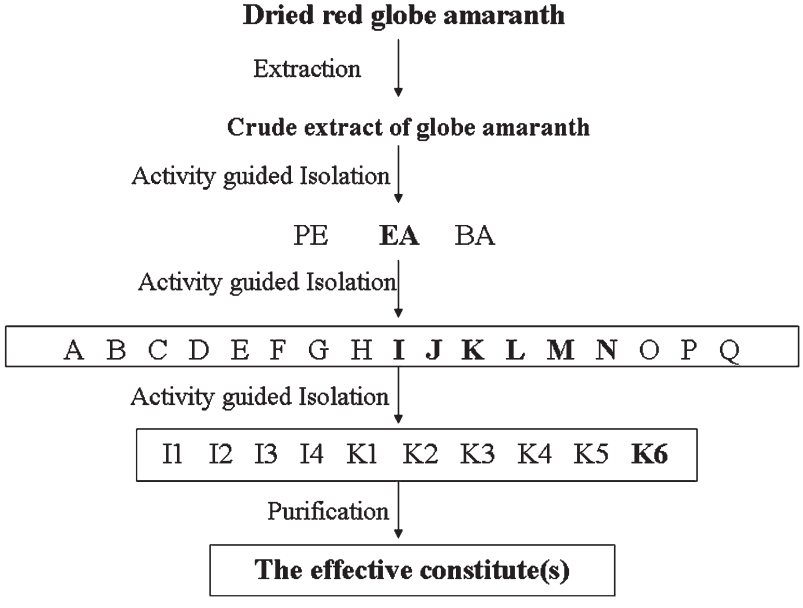

Figure 1. Flow chart of isolation of tyrosinase inhibitors from red globe amaranth.

CIRCULAR DICHROISM MEASUREMENTS

Circular dichroism (CD) spectroscopy can be used to estimate the overall conformation of protein molecules. The CD measurements of tyrosinase in the presence and absence of VA were obtained in the range of 190–250 nm using a 2-mm quartz cuvette at a scan speed of 60 nm/min, with the results from three scans averaged for each CD spectrum. Each 1.0 ml mixture contained 0.9 ml tyrosinase (0.1 mg, dissolved in water) and 0.1 ml VA (dissolved in a 10% methanol aqueous solution). The VA/tyrosinase molar ratio was varied (0, 1:1, and 4:1), and the CD spectra were recorded using MOS-450 spectrometer (Bio-Logics Inc., Grenoble, France) at 25°C (19,20).

ULTRAVIOLET SPECTROSCOPIC MEASUREMENTS

Ultraviolet (UV)/visible spectroscopy was used to evaluate whether VA could chelate copper ion of tyrosinase. Spectra at 240–400 nm were measured using the UV-2102 spectrophotometer (Unico Inc., Shanghai, China). The mixture contained 1.9 ml of the samples (10 μg/ml, dissolved in 0.2% methanol) and 0.1 ml of 50 m*M* phosphate buffer (pH 6.8) with mushroom tyrosinase (100 units/ml). Scans of 1.0 m*M* $CuSO_4$ were obtained for comparison (21,22).

MODEL BUILDING AND MOLECULAR DOCKING

The crystal structure of tyrosinase from *Bacillus megaterium* (TyrBm; PDB ID: 3NQ1) (23) was chosen as the protein model in this study. The dicopper and ligands were removed from 3NQ1 before the docking computation was performed. The docking algorithm was based on the ROSETTALIGAND software (http://www.rosettacommons.org) as previously described (24,25). For each receptor–ligand pair, 500 docking results were generated from the docking calculation. Then, top 10 structures were selected based on the total ROSETTA energy, and they were ranked by the receptor–ligand interaction energy and ligand conformational variation parameters. The figures were produced using the PyMOL molecular graphics system (http://www.pymol.org).

RESULTS AND DISCUSSION

EFFECT OF FRACTIONS FROM RED GLOBE AMARANTH ON TYROSINASE ACTIVITY

Table II shows the inhibitory effect of the crude extracts from red globe amaranth flower on tyrosinase. Table II shows that the crude extract had a concentration-dependent inhibitory effect on tyrosinase activity, with an IC_{50} value of 3.32 mg/ml. These results suggest that the crude extract of red globe amaranth flower has potential inhibitory effects on tyrosinase. The inhibitory effects on tyrosinase by additional EA extract fractions are presented in Table III, which shows that the eight fractions (G–N) inhibited tyrosinase activity to varying degrees. Overall, the fractions I, K, and N could inhibit tyrosinase activity considerably with inhibition rates of 51.05%, 54.37%, and 70.89%,

Table II
Inhibitory Effects of Crude Extracts of the Red Globe Amaranth on Tyrosinase

Concentration (mg/ml)	Inhibition rate (%) (Mean±SD)
0.35	15.43 ± 1.48
1.75	30.47 ± 1.16
3.50	48.91 ± 0.22
5.25	75.81 ± 1.67

respectively; the eluents for these fractions were ether-acetic ether in 8:2, 6:4, and 6:4 ratios, respectively.

Further separation yielded 14 fractions, whose inhibitory effects on tyrosinase are shown in Table III. The K fraction generally showed the greatest inhibition of tyrosinase activity. The K6 fraction was especially suitable for inhibiting tyrosinase activity; it almost inhibited tyrosinase activity at the concentrations tested. Finally, we successfully identified VA from K6 as one of the most effective constituents of the red globe amaranth at depigmenting substrates based on its ability to inhibit tyrosinase activity.

Table III
Inhibitory Effects of the Fractions on Tyrosinase Activity

Fraction	Fraction	Inhibition rate (%) (Mean±SD)
G		40.47 ± 5.46
I		51.05 ± 10.57
	I1	44.26 ± 3.42
	I2	8.36 ± 1.98
	I3	41.89 ± 4.71
	I4	20.07 ± 1.70
J		43.57 ± 1.46
K		54.37 ± 9.43
	K1	4.81 ± 4.70
	K2	48.14 ± 10.34
	K3	36.03 ± 10.93
	K4	49.04 ± 0.26
	K5	58.12 ± 7.36
	K6	96.48 ± 2.17
L		31.85 ± 1.37
M		22.43 ± 4.33
N		70.89 ± 7.58
	N1	31.60 ± 8.95
	N2	36.24 ± 0.19
	N3	46.94 ± 3.07
	N4	23.30 ± 2.12

INHIBITORY EFFECT OF VA ON TYROSINASE

The inhibitory effect of the prepared VA from red globe amaranth on tyrosinase activity is given in Table IV, which shows that VA had a concentration-dependent inhibitory effect on tyrosinase activity. On the basis of linear line-fitting, the IC_{50} values of VA on the activities of tyrosinase monophenolase and diphenolase were 0.53 and 0.63 mg/ml, respectively. Arbutin, which is a commercial tyrosinase inhibitor, can inhibit tyrosinase monophenolase activity; however, it did not inhibit diphenolase activity very well at the doses tested. VA inhibited tyrosinase activity, especially diphenolase activity, to a greater extent than arbutin when the concentration was over 0.67 mg/ml. When the dose of VA was greater than 1.00 mg/ml, the tyrosinase activity was almost inhibited. Moreover, we found that VA inhibited monophenolase activity more effectively than diphenolase activity, especially at the low concentrations of 0.17–0.67 mg/ml used in our study. Thus, VA could potentially be a good inhibitor of tyrosinase activity.

VA was traced from the EA part; other parts of the crude extracts also have tyrosinase inhibitory effect, such as PA and BA, although they are not the major parts, so the abandoned parts may be the reason that the efficacy of highly purified fraction was only five-fold higher than that of crude extract.

EFFECT OF VA ON CONFORMATION OF TYROSINASE

We investigated the structural and conformational changes caused by the addition of VA (26). The CD spectra of tyrosinase in the absence and presence of VA were investigated; the result is shown in Figure 2. The CD results show that the interaction between tyrosinase and VA hardly affects the spectra of tyrosinase in the range of 200–250 nm with two concentrations of the inhibitor, which indicates that VA interacts with tyrosinase without inducing detectable changes in the enzyme conformation.

UV SPECTROSCOPIC ANALYSIS

Tyrosinase is classified as a type-3 copper protein family member with a dicopper (CuA and CuB) center lodged in a helical bundle. The dicopper center has a high degree of conservation and plays an important catalytic role in the activity of tyrosinase (27). When

Table IV
Inhibitory Effects of Vanillic Acid and Arbutin on Tyrosinase (mean value ± standard deviation)

	L-tyrosine as substrate		L-dopa as substrate	
Dose (mg/ml)	VA (Mean±SD)	Arbutin (Mean±SD)	VA (Mean±SD)	Arbutin (Mean±SD)
0.17	8.19 ± 1.35	54.43 ± 0.09	2.08 ± 0.11	8.44 ± 0.77
0.33	30.70 ± 5.32	64.35 ± 1.56	3.33 ± 1.26	10.58 ± 0.68
0.67	77.16 ± 2.10	71.36 ± 2.96	59.67 ± 5.10	7.64 ± 0.93
1.00	97.74 ± 0.23	78.33 ± 0.75	82.06 ± 2.50	12.43 ± 1.27
1.33	98.83 ± 0.54	79.60 ± 1.09	90.92 ± 0.55	16.77 ± 1.73

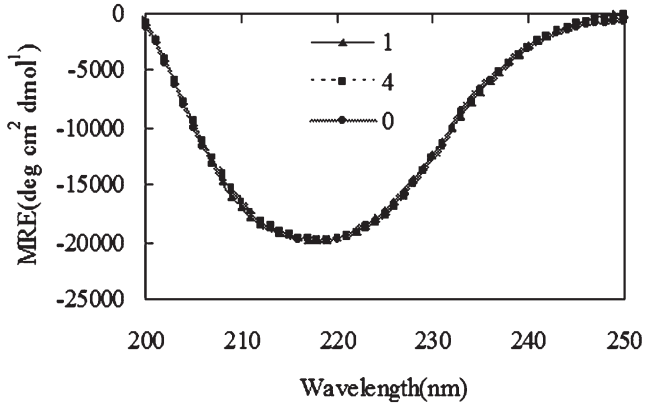

Figure 2. CD spectroscopy of tyrosinase with the addition of VA.

inhibitors with conjugative effect interact with Cu^{2+}, which can enhance the interior conjugation effect of the inhibitor, the spectral characteristics of the inhibitors will show red shift peaks. As a result, in research on the mechanism of tyrosinase inhibitors , UV/visible spectroscopy can be used for studying the chelate formation between the copper ions of tyrosinase and inhibitors. Kubo and Kinst-Hori reported that kaempferol could inhibit tyrosinase activity as a copper chelator, and the inhibitory mechanism was demonstrated by a bathochromic shift of the spectral characteristics of kaempferol after adding excessive Cu^{2+} (21). Kim *et al.* found that new peaks of a flavonoid were produced on interaction with the Cu^{2+} and concluded that the flavonoid could inhibit the tyrosinase interacting with the copper ion of the enzyme (22). Figure 3 shows the changes in the UV/visible spectra of VA after the addition of tyrosinase and excess Cu^{2+}. In the UV/visible spectrum, VA had characteristic absorption bands at 255 and 288 nm, which are

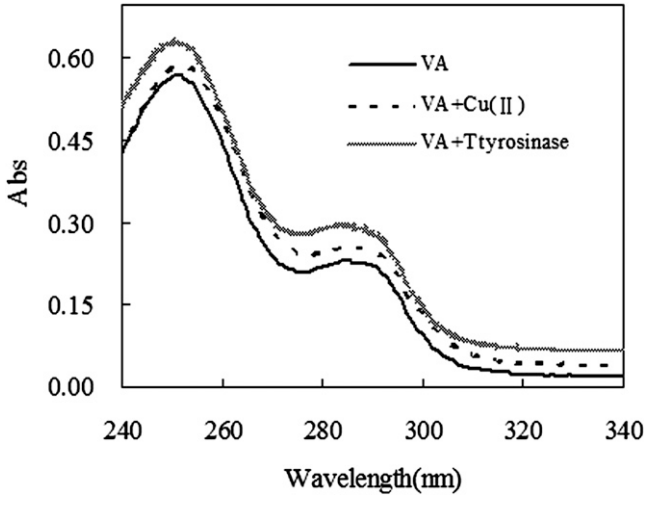

Figure 3. UV/visible spectrum of VA with the addition of Cu^{2+} and tyrosinase.

assumed to be band K (210–250 nm) and band B (260–300 nm) of a benzene ring. The maximum absorptions of VA remained the same after the addition of excess Cu^{2+}, whereas the absorption maxima shifted to 249 and 285 nm after the addition of tyrosinase. These results illustrate that the VA can interact with tyrosinase; however, chelation interaction between VA and the dicopper copper ion of the enzyme is not included (30).

STEREOSCOPIC STRUCTURAL HOMOLOGY ANALYSIS

The conformations of VA docked onto tyrosinase were investigated to determine the mechanism of inhibition of mushroom tyrosinase by VA. Because a three-dimensional structure of mushroom tyrosinase has not yet been reported, we used crystal structure of tyrosinase from *B. megaterium* as a model (Figure 4, dark) (23). Before the molecular docking was performed, the structure of mushroom tyrosinase (TyrMu) (Figure 4, light) was predicted according to its primary sequence (GenBank ID: CAC82195.1) from the Phyre Server (28) for comparison. We superimposed the predicted structure of TyrMu with the crystal structure of TyrBm using the secondary structure matching superimposition program Coot (29). The superimposition results of the overall structures and the active sites are shown in Figure 4. The predictions indicated that the catalytic core domains of the two three-dimensional structures are highly conserved. Therefore, it is reasonable to choose the active center of TyrBm to serve as our structural model.

MOLECULAR DOCKING ANALYSIS

The molecular simulations of the interaction between VA and tyrosinase are shown in Figure 5. VA was bound by interactions with residues Glu192 and Gly213 (Glu195 and Gly216 in TyrBm) at the entrance to the active center and His57 (His60 in TyrBm) in the active center (Figure 5A). Thus, the conformation of the active pocket may be changed by VA as a result of the interaction with adjacent residues (23). Furthermore, we

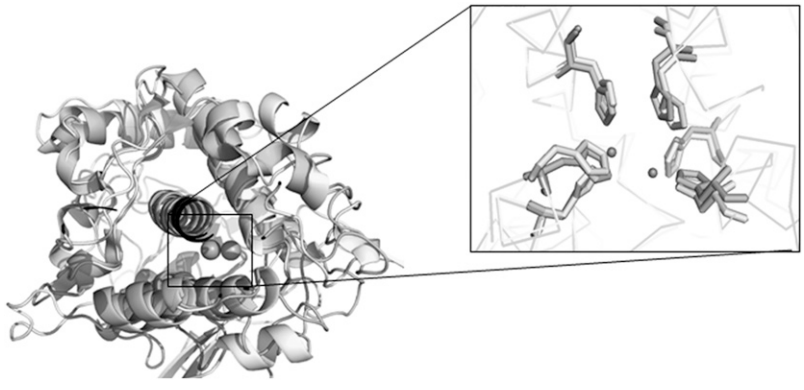

Figure 4. Superimposition of TyrBm (dark) and the prediction of the mushroom tyrosinase structure (light). The two balls were dicopper center of tyrosinase.

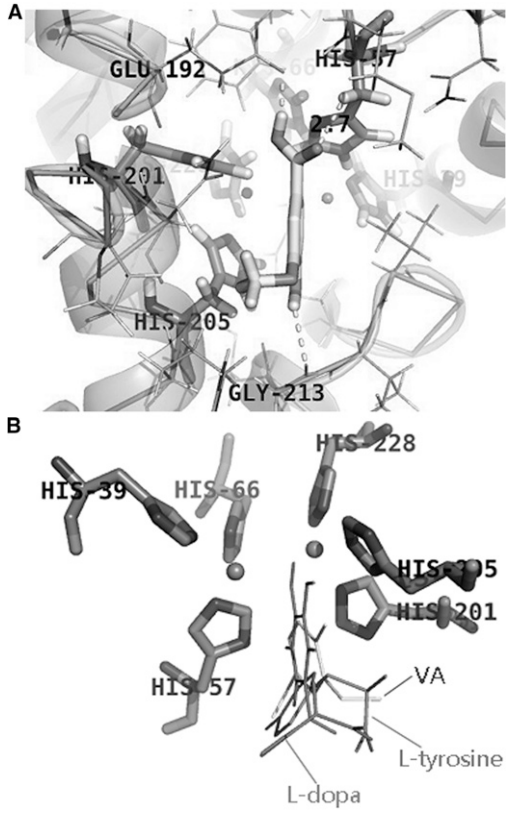

Figure 5. Suggested docking model for VA and tyrosinase. (A) Interaction of VA and tyrosinase in the docking model. (B) Superimposition of VA with L-tyrosine and L-dopa.

superimposed VA with substrates in PyMOL (Figure 5B). The overlap prediction indicates that the three-dimensional position occupied by VA is almost the same as that of the substrates at the tyrosinase active core domain. Thus, VA obstructs the correct orientation of the substrates at the catalytic center, which suggests one possible mechanism of inhibition (23). Sendovski *et al.* suggested that His57 (His60 in TyrBm) is responsible for the deprotonation of the monophenol substrate (23). The interaction of VA with His57 implies that VA may have a greater effect on monophenolase activity than on diphenolase activity, which is consistent with the results described above.

For the modeling of molecular docking using Rosetta, the value of the total score is related to the free energy of the receptor–ligand complex. The total scores were −936.57, −934.99, and −936.46 for the modeling of docking with VA, L-tyrosine, and L-dopa, respectively. Thus, the tyrosinase–VA complex exhibited greater stability compared with that of the substrate complexes. Thus, VA may bind to tyrosinase more easily and more strongly than monophenol and diphenol substrates. As a result, VA could inhibit tyrosinase activity in the presence of substrates, as shown in Table IV. In addition, because the tyrosinase–L-tyrosine complex is the least stable, the competition by the inhibitor may be stronger for monophenol substrate, which may be another reason that the monophenolase activity is lower than the diphenolase activity in the presence of VA.

CONCLUSION

As a Chinese herbal medicine, red globe amaranth strongly inhibits tyrosinase activity. In addition, we identified for the first time that VA is a constituent of amaranth with strong tyrosinase inhibition activity. As a potential tyrosinase inhibitor, VA could inhibit both the monophenolase and diphenolase activities of tyrosinase better than the commercial tyrosinase inhibitor arbutin. We found that VA did not change the overall conformation of the enzyme structure and did not chelate the dicopper when it interacted with tyrosinase. The most probable mechanism of inhibition is that VA interacts with tyrosinase more stably than the substrates. When VA interacts with tyrosinase, the path for the substrates to the enzyme catalytic center is obstructed. Therefore, the orientation of the substrates to the dicopper center is interrupted because of the hindering effect, which inhibits the monophenolase and diphenolase activities of tyrosinase. However, the interaction model and molecular mechanism were predicted according to the docking algorithm, which is limited to simulating the interaction of a protein and a ligand. Protein crystallography studies may provide further insight into the molecular mechanism of inhibition.

ACNOWLEDGMENTS

We acknowledge the financial support from the National Natural Science Fund of China (Grant Nos 31130042 and 31171630), the Fundamental Research Funds for the Central Universities, SCUT (Grant No. 2012ZG0007), and the Program for New Century Excellent Talents in University (Grant No. NCET-10-0362). Dr. Wei Luo is warmly thanked for excellent technical assistance.

REFERENCES

(1) Y.J. Kim and H. Uyama, Tyrosinase inhibitors from natural and synthetic sources: Structure, inhibition mechanism and perspective for the future, *Cell. Mol. Life Sci.*, **62,** 1707–1723 (2005).
(2) S. Parvez, M. Kang, H.S. Chung, C. Cho, M.C. Hong, M.K. Shin, and H. Bae, Survey and mechanism of skin depigmenting and lightening agents, *Phytother. Res.,* **20,** 921–934 (2006).
(3) G.M. Casanola-Martin, Y. Marrero-Ponce, M.T. Khan, A. Ather, K.M. Khan, F. Torrens, and R. Rotondo, Dragon method for finding novel tyrosinase inhibitors: Biosilico identification and experimental in vitro assays, *Eur. J. Med. Chem.,* **42,** 1370–1381 (2007).
(4) Y. Ryu, I. Westwood, N. Kang, H. Kim, J. Kim, Y. Moon, and K. Park, Kurarinol, tyrosinase inhibitor isolated from the root of Sophora flavescens, *Phytomedicine,* **15,** 612–618 (2008).
(5) T.S. Chang, H.Y. Ding, S.S.K. Tai, and C.Y. Wu, Mushroom tyrosinase inhibitory effects of isoflavones isolated from soygerm koji fermented with Aspergillus oryzae BCRC 32288, *Food Chem.,* **105,** 1430–1438 (2007).
(6) L. Qiu, Q.X. Chen, Q. Wang, H. Huang, and K.K. Song, Irreversibly inhibitory kinetics of 3, 5-dihydroxyphenyl decanoate on mushroom (*Agaricus bisporus*) tyrosinase. *Bioorg. Med. Chem.,* **13,** 6206–6211 (2005).
(7) L. Qiu, Q.H. Chen, J.X. Zhuang, X. Zhong, J.J. Zhou, Y.J. Guo, and Q.X. Chen, Inhibitory effects of [alpha]-cyano-4-hydroxycinnamic acid on the activity of mushroom tyrosinase, *Food Chem.,* **112,** 609–613 (2009).
(8) K.H. Park, Y.D. Park, J.R. Lee, H.S. Hahn, S.J. Lee, C.D. Bae, J.M. Yang, D.E. Kim, and M.J. Hahn, Inhibition kinetics of mushroom tyrosinase by copper-chelating ammonium tetrathiomolybdate, *Biochim. Biophys. Acta. Gen. Subj.,* **1726,** 115–120 (2005).
(9) P. Han, C.Q. Chen, C.L. Zhang, K.K. Song, H.T. Zhou, and Q.X. Chen, Inhibitory effects of 4-chlorosalicylic acid on mushroom tyrosinase and its antimicrobial activities, *Food Chem.,* **107,** 797–803 (2008).

(10) C.K. Hsu, C.T. Chang, H.Y. Lu, and Y.C. Chung, Inhibitory effects of the water extracts of Lavendula sp. on mushroom tyrosinase activity, *Food Chem.*, **105,** 1099–1105 (2007).
(11) Y.M. Chung, H.C. Wang, M. El-Shazly, Y.L. Leu, M.C. Cheng, C.L. Lee, F.R. Chang, and Y.C. Wu, Antioxidant and tyrosinase inhibitory constituents from the desugared sugarcane extract, a by-product of sugar production, *J. Agric. Food Chem.*, **59,** 9219–9225 (2011).
(12) B. Dinda, B. Ghosh, S. Arima, N. Sato, and Y. Harigaya, Phytochemical investigation of *Gomphrena globosa* aerial parts, *Incl. Med. Chem.*, **43,** 2223–2227 (2004).
(13) F. Ferreres, A. Gil-Izquierdo, P. Valentao, and P.B. Andrade, Structural characterization of phenolics and betacyanins in *Gomphrena globosa* by high-performance liquid chromatography-diode array detection/electrospray ionization multi-stage mass spectrometry, *Rapid Commun. Mass Spectrom.,* **25,** 3441–3446 (2011).
(14) V. Kahn, N. BenShalom, and V. Zakin, Effect of benzoic acid and some of its derivatives on the rate of DL-DOPA oxidation by mushroom tyrosinase, *J. Food Biochem.*, **21,** 125–143 (1997).
(15) M. Miyazawa, T. Oshima, K. Koshio, Y. Itsuzaki, and J. Anzai, Tyrosinase inhibitor from black rice bran, *J. Agric. Food Chem.,* **51,** 6953–6956 (2003).
(16) T.H. Chou, H.Y. Ding, W.J. Hung, and C.H. Liang, Antioxidative characteristics and inhibition of alpha-melanocyte-stimulating hormone-stimulated melanogenesis of vanillin and vanillic acid from Origanum vulgare, *Exp. Dermatol.*, **19,** 742–750 (2010).
(17) A. Lai, M. Monduzzi, and G. Saba, Carbon-13 NMR studies on catechol, phenol and benzene derivatives of biological relevance, *Magn. Reson. Chem.,* **23,** 379–383 (1985).
(18) C.K. Lee, C.K. Lu, Y.H. Kuo, J.Z. Chen, and G.Z. Sun, New prenylated flavones from the roots of Ficus beecheyana, *J. Chin. Chem. Soc. (Taipei, Taiwan),* **51,** 437–442 (2004).
(19) S. Shaikh, J. Seetharamappa, P. Kandagal, and S. Ashoka, Binding of the bioactive component isothipendyl hydrochloride with bovine serum albumin, *J. Mol. Struct.,* **786,** 46–52 (2006).
(20) W. Song, M. Ao, Y. Shi, L. Yuan, X. Yuan, and L. Yu, Interaction between phillygenin and human serum albumin based on spectroscopic and molecular docking, *Spectrochim. Acta, Part A,* **85,** 120–126 (2012).
(21) I. Kubo and I. Kinst-Hori, Flavonols from saffron flower: Tyrosinase inhibitory activity and inhibition mechanism, *J. Agric. Food Chem.,* **47,** 4121–4125 (1999).
(22) D. Kim, J. Park, J. Kim, C. Han, J. Yoon, N. Kim, J. Seo, and C. Lee, Flavonoids as mushroom tyrosinase inhibitors: A fluorescence quenching study, *J. Agric. Food Chem.,* **54,** 935–941 (2006).
(23) M. Sendovski, M. Kanteev, V.S. Ben-Yosef, N. Adir, and A. Fishman, First structures of an active bacterial tyrosinase reveal copper plasticity, *J. Mol. Biol.*, **405,** 227–237 (2010).
(24) I.W. Davis and D. Baker, RosettaLigand docking with full ligand and receptor flexibility, *J. Mol. Biol.,* **385,** 381–392 (2009).
(25) J. Meiler and D. Baker, ROSETTALIGAND: Protein-small molecule docking with full side-chain flexibility, *Proteins: Struct., Funct., Bioinf.*, **65,** 538–548 (2006).
(26) X. Wu, J. Liu, Q. Wang, W. Xue, X. Yao, Y. Zhang, and J. Jin, Spectroscopic and molecular modeling evidence of clozapine binding to human serum albumin at subdomain IIA, *Spectrochim. Acta, Part A,* **79,** 1202–1209 (2011).
(27) Y. Matoba, T. Kumagai, A. Yamamoto, H. Yoshitsu, and M. Sugiyama, Crystallographic evidence that the dinuclear copper center of tyrosinase is flexible during catalysis, *J. Biol. Chem.,* **281,** 8981 (2006).
(28) L.A. Kelley and M.J.E. Sternberg, Protein structure prediction on the Web: A case study using the Phyre server, *Nat. Protoc.,* **4,** 363–371 (2009).
(29) E. Krissinel and K. Henrick, Secondary-structure matching (SSM), a new tool for fast protein structure alignment in three dimensions, *Acta Crystallogr., Sect D: Biol. Crystallogr.,* **60,** 2256–2268 (2004).
(30) Y.X. Si, S.J. Yin, D. Park, H.Y. Chung, L. Yan, Z.R. Lv, H.M. Zhou, J.M. Yang, G.Y. Qian, and Y.D. Park, Tyrosinase inhibition by isophthalic acid: kinetics and computational simulation, Int. *J. Biol. Macromol.*, **48,** 700–704 (2011).